Hindawi
International Journal of Antennas and Propagation
Volume 2023, Article ID 2926111, 8 pages
https://doi.org/10.1155/2023/2926111

Research Article

Synthesis of Sparse Uniformly Excited Concentric Ring Arrays Using the Chaos Sparrow Search Algorithm

Bin Wang, Xue Tian, and Kui Tao

College of Electronic Engineering & Institute for Advanced Science, Chongqing University of Posts and Telecommunications, Chongqing 400065, China

Correspondence should be addressed to Bin Wang; wangbin1@cqupt.edu.cn

Received 3 March 2023; Revised 10 April 2023; Accepted 23 April 2023; Published 16 May 2023

Academic Editor: Mohammad Hassan Neshati

In this paper, an effective synthesis method for sparse uniformly excited concentric ring array (CRA) element positions featuring a minimum sidelobe level (SLL) is presented. This method is based on the chaos sparrow search algorithm (CSSA), which can search for the optimal solution under multiple constraints. By improving the constraint on the number of array elements on each ring, the solution range of the optimal solution is further reduced, and the global search ability of the algorithm is effectively improved by introducing tent mapping into the algorithm to initialize the population. Numerical examples are presented to assess the effectiveness and reliability of the proposed method, showing that it can achieve better results than existing methods in the design of sparse concentric ring array arrangements.

1. Introduction

Concentric ring array (CRA), which has the symmetrical structure of a circular array, ensures that its beam and antenna gain performance are basically maintained in a certain range, and it can relatively achieve mutual coupling balance. These excellent properties have made it the subject of intensive investigations in recent years [1–4]. In particular, array synthesis patterns with arbitrary element positions have attracted more attention [5, 6]. Compared with a uniform array antenna with the same aperture, the sparse array antenna can achieve the same resolution with fewer array elements; then, the cost of the antenna system is reduced [7]. At the same time, sparse array antennas can achieve a low sidelobe level (SLL) without amplitude weighting. In the synthesis of sparse uniformly excited concentric ring arrays, the location of the element is an important factor in the optimal performance because of its ability to obtain the minimum peak sidelobe level (PSLL), but it also leads to complex nonlinear optimization problems [8, 9].

To solve the nonlinear problem of sparse uniformly excited concentric ring array design, several synthesis techniques have been proposed. A method based on space tapering has been suggested by Willey [10], which can be used by controlling the element density taper to match the amplitude taper of the minimum SLL. For the fast synthesis of CRA, a deterministic approach that takes inspiration from density-tapered techniques to optimize the location of array elements has been presented in [11, 12]. The normalized Taylor amplitude taper of the conventional filled array was considered a distribution function to determine the location of the array elements. However, the results obtained by analytical methods are often not globally optimal, and their applications in array synthesis are mostly limited to the suppression of sidelobes. With the advent of intelligent optimization methods, such as genetic algorithms (GAs) [13–16], particle swarm optimization (PSO) [17], and differential evolution (DE) [18], they have been successfully applied to the synthesis of sparse CRA due to their global search capability. A hybrid approach (HA) for CRA synthesizing to suppress the PSLL has been proposed in [19], which is convenient for synthesizing uniform amplitude concentric ring arrays with certain constraints. Although intelligent optimization algorithms have the advantage of solving sparse array nonlinear synthesis and achieving better

optimization results, their solving efficiency is low, and it is easy to fall into a local optimum.

The sparrow search algorithm (SSA) imitates the foraging and antipredation behavior of sparrows [20], which has the advantages of high search accuracy, strong versatility, and easy implementation compared with other intelligent algorithms [21, 22]. To improve the global search ability and prevent falling into the local optimal solution, a chaos sparrow search algorithm (CSSA) is proposed by introducing a tent-mapping chaos operator into the SSA, which effectively guarantees the uniformity of the initial population and enhances population diversity. This method achieves the suppression of PSLL by optimizing the position distribution of uniformly excited CRA elements. The simulation results demonstrate the effectiveness and superiority of the proposed method.

The paper is organized as follows: Section 2 formulates the problem, and Section 3 describes the procedure of synthesis. Numerical examples and results are presented in Section 4 to fully demonstrate the effectiveness and superiority of this proposed method. Finally, Section 5 concludes this paper.

2. Synthesis of CRA

In Figure 1, a sparse concentric array with a single element at the center and N_r rings from the center to the edge is shown, and the starting element of each ring is arranged on the X-axis. The radius of each ring is r_n, and the number of elements on the corresponding ring is N_n. Generally, the array factor can be characterized as follows [19]:

$$AF(\theta,\varphi) = 1 + \sum_{n=1}^{N_r}\sum_{m=1}^{N_n} e^{jkr_n\sin\theta\cos(\varphi-\varphi_{mn})}, \tag{1}$$

where k is the wave number, $k = 2\pi/\lambda$, λ is the operating wavelength, φ_{mn} is the angular position of the mth element in the nth ring, $\varphi_{mn} = 2\pi(m-1)/N_n$, and φ and θ are the azimuth and elevation angles, respectively.

Assuming that the diameter of the outer ring is D, the minimum spacing of array elements is $d_{\min}$. To improve the search efficiency, all elements of the array need to satisfy the minimum spacing constraint between adjacent elements and the maximum aperture constraint:

$$\begin{cases} r_n = nd_{\min} + \Delta r_n, n = 1, 2, \cdots, N_r, \\ r_{N_r} = \dfrac{D}{2}, \\ 0 \le \Delta r_i \le \Delta r_j \le \dfrac{D}{2} - N_r d_{\min}, 1 \le i < j \le N_r. \end{cases} \tag{2}$$

The array radius vector $\mathbf{R} = \{r_1, r_2, \cdots, r_{N_r}\}$ can be represented as follows [19]:

$$\mathbf{R} = \mathbf{C} + \Delta\mathbf{R}, \tag{3}$$

where $\mathbf{C} = \{d_{\min}, 2d_{\min}, \cdots, N_r d_{\min}\}$ is the constant part and $\Delta\mathbf{R} = \{\Delta r_1, \Delta r_2, \cdots \Delta r_{N_r}\}$ is the variable part.

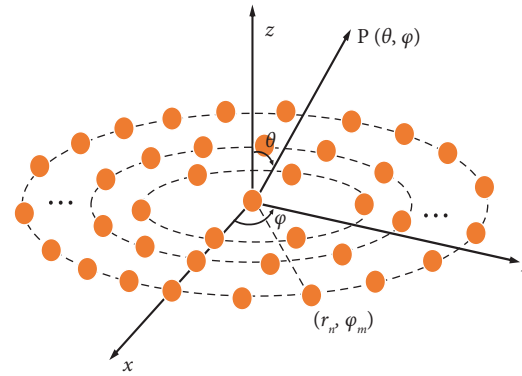

Figure 1: Geometry of a sparse concentric ring array.

After determining the ring radius, the maximum number of array elements $N_{n\max}$ on a ring can be expressed by the ring radius r_n and minimum array element spacing $d_{\min}$ as follows [13]:

$$N_{n\max} = \left\lfloor \frac{2\pi r_n}{d_{\min}} \right\rfloor. \tag{4}$$

Theoretically, N_n can be any integer between 1 and $N_{n\max}$, but the scarcity of array elements will result in array directivity and gain losses. Therefore, constraints should be set to the minimum number of array elements on the ring. To make the element distribution of the sparse array satisfy the feature of gradual sparsity from the center to the edge, N_n on the sparse array is expressed as

$$\begin{cases} N_n = \lfloor N_{n\min} + (N_{n\max} - N_{n\min}) \cdot k_n \rfloor, \\ N_{n\min} = \dfrac{N_{n\max}}{3} + \left(2\dfrac{N_{n\max}}{3}\right) \cdot \mathrm{rand}(0,1), \end{cases} \tag{5}$$

where k_n is the sparse coefficient, which is used to control the sparse rate of elements on each ring, k_n is determined by the amplitude distribution on the corresponding full-array ring, i.e., sparse coefficient $k_n = \{I_1, I_2, \cdots, I_{N_r}\}$, and $N_{n\min}$ is the minimum number of array elements on the ring. To increase the optimization space of N_n, $N_{n\min}$ is set to a random number between $N_{n\max}/3$ and $N_{n\max}$.

The fitness function is defined as follows [19]:

$$\mathrm{PSLL}(r, N_n) = \max\left\{\left|\frac{AF(\theta,\varphi)}{AF_{\max}}\right|\right\}, 0 < \theta_{\min} < \theta \le \frac{\pi}{2}, \tag{6}$$

where $AF(\theta,\varphi)$ represents the array factor, $AF_{\max}$ is the maximum value of the main beam, and $\theta_{\min}$ is position of the first null point.

3. CSSA Analysis

To improve the efficiency of the convergence performance of the sparse concentric ring array optimization problem while reducing the PSLL, the CSSA is used to solve the synthesis of sparse concentric ring arrays. Since the position updating of the CSSA is jumpy and discontinuous, the local optimum can be effectively avoided. The specific optimization steps are as follows.

Step 1. Population initialization.

Assuming that the SSA involves a group of N_P sparrows with a spatial dimension dim, the position distribution of sparrows can be expressed as

$$\begin{bmatrix} \Delta\mathbf{R}_1 \\ \Delta\mathbf{R}_2 \\ \vdots \\ \Delta\mathbf{R}_{N_p} \end{bmatrix} = \begin{bmatrix} x_{1,1} & x_{1,2} & \cdots & x_{1,\dim} \\ x_{2,1} & x_{2,2} & \cdots & x_{2,\dim} \\ \vdots & \vdots & \ddots & \vdots \\ x_{N_p,1} & x_{N_p,2} & \cdots & x_{N_p,\dim} \end{bmatrix}. \tag{7}$$

To improve the global search ability of the algorithm and avoid the decline of population diversity in later iterations, tent mapping is chosen as the initialized population for the chaotic sequence of the optimization algorithm. The chaotic self-mapping of the tent is represented as

$$Z_{i+1} = \begin{cases} 2Z_i, 0 \le Z \le \dfrac{1}{2}, \\ \\ 2\left(1 - Z_i\right), \dfrac{1}{2} < Z \le 1, \end{cases} \tag{8}$$

which can be abbreviated as

$$Z_{i+1} = \left(2Z_i\right) \bmod 1. \tag{9}$$

Random variables are introduced to the tent mapping to prevent the destruction of the randomness, ergodicity, and regularity of chaotic variables:

$$Z_{i+1} = \left(2Z_i\right) \bmod 1 + \frac{\operatorname{rand}(0,1)}{N_P T}, \tag{10}$$

where T is the maximum number of iterations.

After the chaotic variable is generated by (10), it is introduced to the solution space of variables, and the initial population is generated as

$$x = l_{\mathrm{b}} + \left(U_{\mathrm{b}} - l_{\mathrm{b}}\right) \cdot Z_d, \tag{11}$$

where l_b and U_b are the minimum and maximum values of x, respectively.

Step 2. Population update based on the SSA.

In the SSA, a discoverer-joiner sparrow population model is established, and some sparrows are randomly selected as guards. The discoverer position update formula is as follows [22]:

$$x_{i,j}^{t+1} = \begin{cases} x_{i,j}^{t} \cdot \exp\left(\dfrac{-i}{\alpha \cdot T}\right), R_1 < \mathrm{ST}, \\ \\ x_{i,j}^{t} + Q \cdot \mathbf{L}, R_1 \ge \mathrm{ST}, \end{cases} \tag{12}$$

where $x_{i,j}^{t}$ is the position of the ith sparrow of the tth generation in the jth dimension, α is a uniform random number in (0, 1], T is the maximum number of iterations, $R_1 \in [0, 1]$ indicates the warning value, $ST \in [0.5, 1.0]$ indicates the alert threshold, Q is a random number satisfying the standard normal distribution, and $\mathbf{L}$ is a matrix of $1 \times \dim$ whose elements are all 1. When $R_1 < ST$, the sparrow population is in a safe state, and the discoverer continues to forage. When $R_1 \ge ST$, danger is found, and all sparrows must fly to safety immediately.

In addition to discoverers, the remaining sparrows in the population are joiners, and their position update formula is as follows [21]:

$$x_{i,j}^{t+1} = \begin{cases} Q \cdot \exp\left(\dfrac{x_{\mathrm{worst},j}^{t} - x_{i,j}^{t}}{i^2}\right), \text{if } i > \dfrac{N_p}{2}, \\ \\ x_p^{t+1} + \left|x_{i,j}^{t} - x_p^{t+1}\right| \cdot A^{+} \cdot \mathbf{L}, \text{otherwise}, \end{cases} \tag{13}$$

where x_P is the best position of the discoverers and x_{worst} indicates the global worst position in the current iteration. When $i > N_p/2$, it means that the ith joiner needs to change its search area to continue searching for food. Conversely, it means that the ith joiner converges to the global optimal position and performs random foraging around.

The formula for updating the position of the guard position is as follows [21]:

$$x_{i,j}^{t+1} = \begin{cases} x_{\mathrm{best}}^{t} + \beta \cdot \left|x_{i,j}^{t} - x_{\mathrm{best},j}^{t}\right|, \text{if } f_i > f_g, \\ \\ x_{i,j}^{t} + K \cdot \left(\dfrac{\left|x_{i,j}^{t} - x_{\mathrm{worst},j}^{t}\right|}{\left(f_i - f_w\right) + \varepsilon_0}\right), \text{if } f_i = f_g, \end{cases} \tag{14}$$

where x_{best} is the current global best position, β is a step control parameter satisfies a distribution of N (0, 1), K is a random number between [−1, 1], ε_0 is a very small constant to avoid zero denominators, f_i is the fitness value of the individual sparrow at present, and f_g and f_w are the best and worst fitness values at present, respectively. The position of these sparrows is random at first. When $f_i > f_g$, the sparrows are vulnerable to predators at the edge of their foraging area. When $f_i = f_g$, it suggests that sparrows at the center of the group are conscious of the danger and demand to approach others quickly to adjust their foraging strategies.

4. Numerical Examples and Results

To validate the superiority and stability of the proposed sparse array synthesis method based on the CSSA, we show three examples of unequally spaced concentric ring arrays with different array apertures, where 100 independent runs for each case are conducted. In all experiments, the antenna elements are rotationally symmetric on the rings, the minimum element spacing $d_{\min}$ is set to 0.5λ, and the CRA's amplitude is equal. In the algorithm, the proportion factor of the number of discoverers to the population $P_N = 0.8$, the guard scale factor $Q_N = 0.2$, and the safety value ST = 0.8 in (12).

4.1. Example A: $R = 4.98\lambda$. In the first example, the array including a total of 8 concentric rings with an array radius of 4.98λ is considered, and the distributed antenna elements are equally spaced on each ring to form an annular grid array. The population size is 100, and the number of

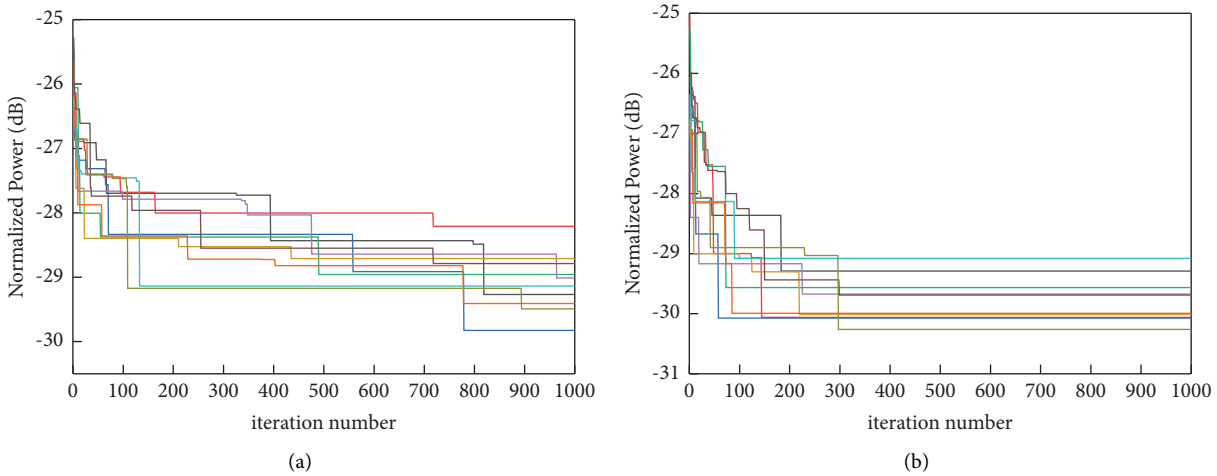

Figure 2: Adaptability curve of 10 independent experiments: (a) SSA; (b) CSSA.

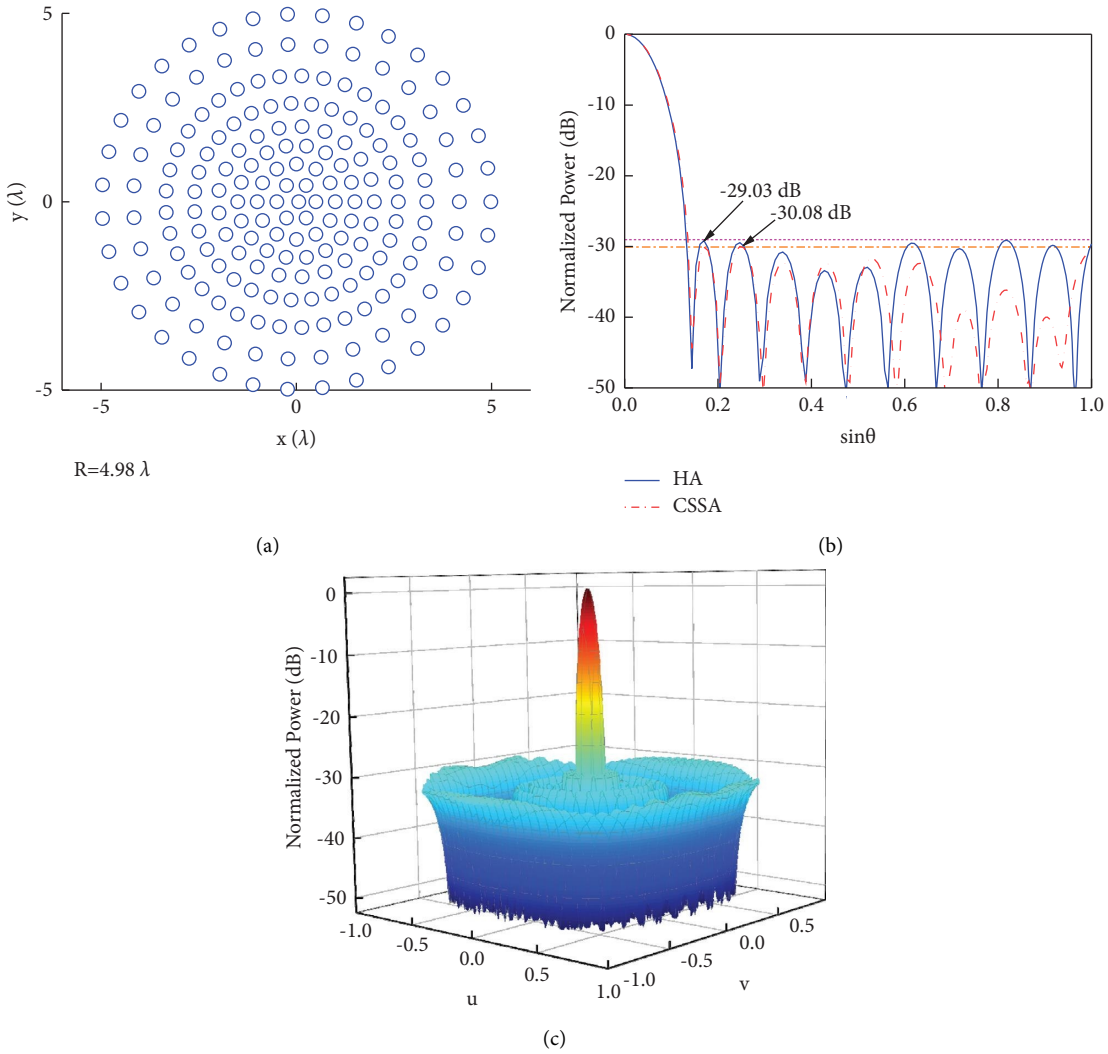

Figure 3: Array synthesis results obtained by CSSA for array aperture $R = 4.98\lambda$: (a) element position; (b) radiation pattern in the $\varphi = 0$ plane; (c) 3-D view of the radiation pattern.

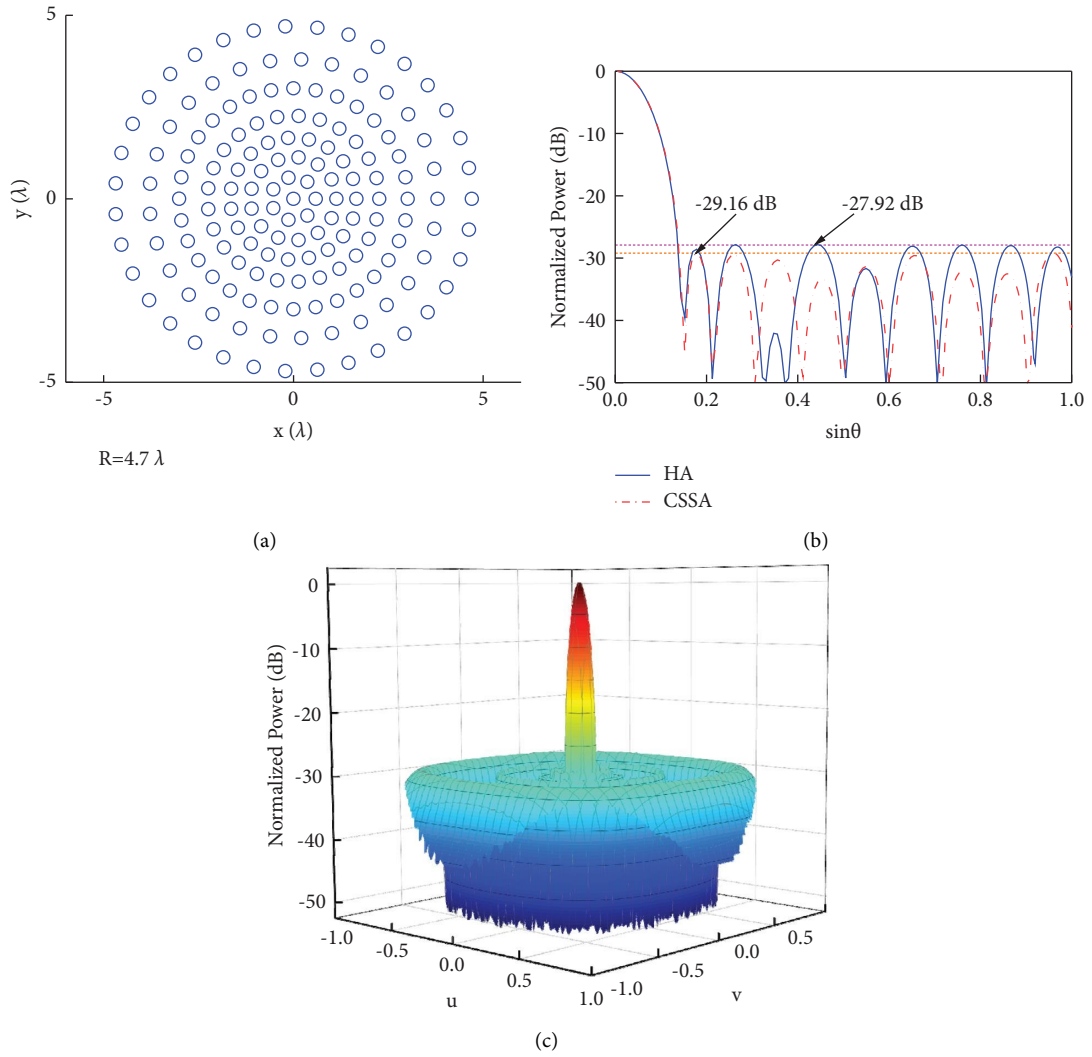

FIGURE 4: Array synthesis results obtained by CSSA for array aperture $R = 4.7\lambda$: (a) element position; (b) radiation pattern in the $\varphi = 0$ plane; (c) 3-D view of the radiation pattern.

generations is 1000. An eight-ring uniform array is used as the original reference array, and a Taylor distribution of −30 dB is chosen as the array excitation function; then, the sparse coefficient $k_n = \{0.98, 0.91, 0.81, 0.70, 0.57, 0.46, 0.38, \text{and } 0.34\}$.

Figures 2(a) and 2(b) show the adaptation curves of the SSA and CSSA for 10 independent experiments, respectively. It can be seen that the adaptation curve of the CSSA converges faster and has better convergence than the SSA. The value of the optimal solution obtained from 10 independent experiments using the SSA ranged from −28.21 dB to −29.83 dB, with an average value of −29.08 dB. The value of the optimal solution obtained from 10 independent experiments using the CSSA ranged from −29.08 dB to −30.07 dB, with an average value of −29.77 dB, which is about 0.69 dB lower than that of the SSA. The results show that the CSSA has better stability than the SSA. Although Figure 2(b) shows that nearly 500 iterations are necessary to reach convergence, numerical results suggested that after 500 iterations, performance remains good. Therefore, the maximum number of iterations $T = 500$ is chosen in the later numerical experiments.

Figure 3(a) shows the optimal element distribution of an acquired array with a single element at the center in 100 independent trials. It has 8 rings with 192 elements. The radius of each ring is 0.50λ, 1.00λ, 1.50λ, 2.00λ, 2.61λ, 3.34λ, 4.17λ, and 4.98λ. The corresponding number of elements is 6, 12, 18, 21, 31, 37, 31, and 35. Figure 3(b) shows the radiation pattern in the $\varphi = 0$ plane, and the PSLL is −30.08 dB, which is better than when using GA (−22.94 dB) [13], MGA (−23.74 dB) [14], and HA (−29.03 dB) [19]. The 3 dB main beamwidth obtained by the CSSA is 0.1129, which is slightly wider than HA (0.1126) [19]. The radiation pattern in three dimensions is illustrated in Figure 3(c). Finally, the total computation time for 500 iterations to complete a single trial is approximately 512 s on a laptop with 8 GB RAM running MATLAB R2019b.

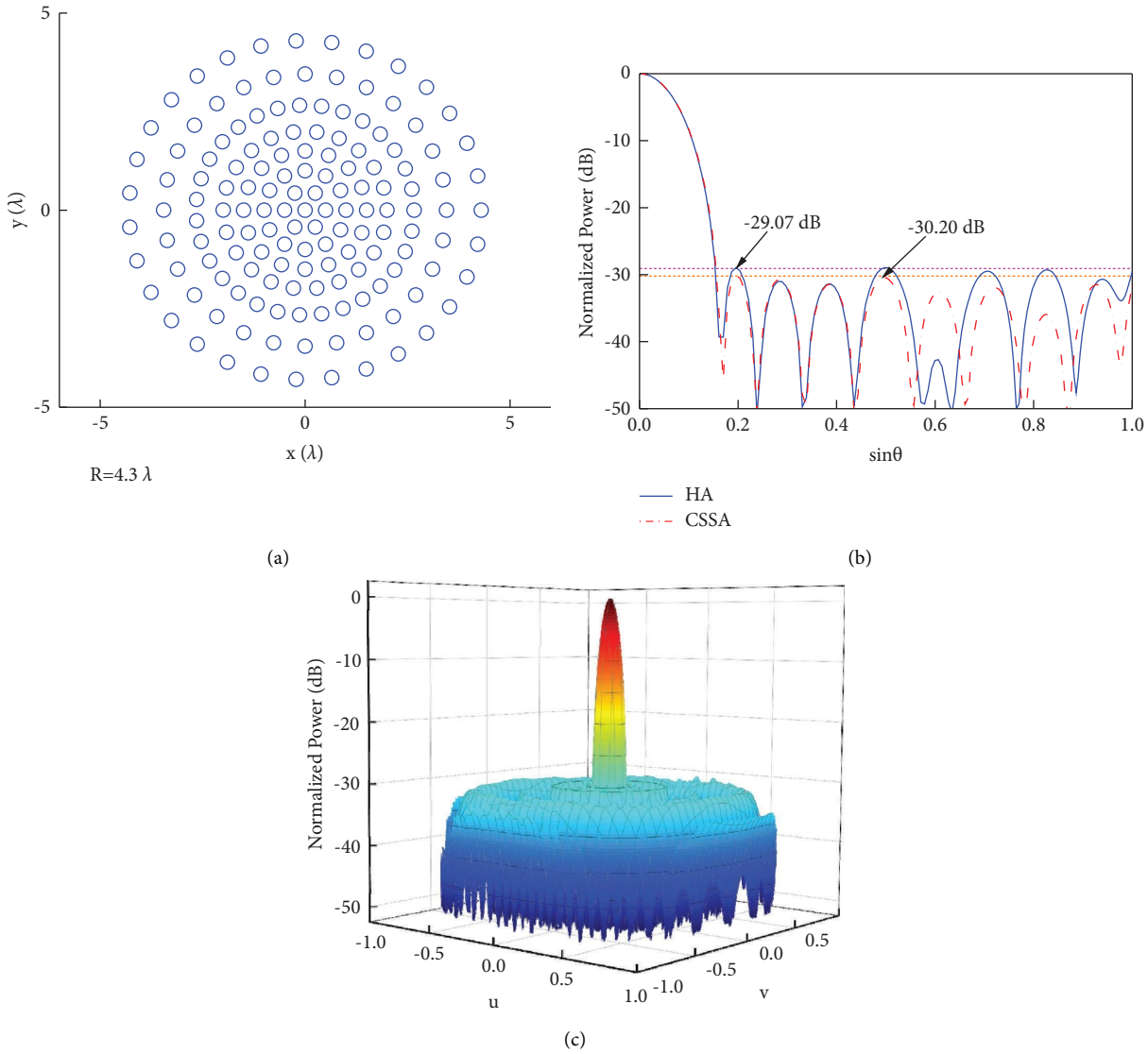

FIGURE 5: Array synthesis results obtained by CSSA for array aperture $R = 4.3\lambda$: (a) element position; (b) radiation pattern in the $\varphi = 0$ plane; (c) 3-D view of the radiation pattern.

4.2. Example B: $R = 4.7\lambda$. Another synthesis experiment with an array radius of 4.7λ has been conducted with the proposed CSSA. A seven-ring uniform array is used as the original reference array, and a Taylor distribution of −30 dB is chosen as the array excitation function; then, the sparse coefficient $k_n = \{0.97, 0.89, 0.77, 0.63, 0.50, 0.39, \text{and } 0.34\}$. We compared the CSSA with the GA and HA, respectively. GA [13] obtained the best PSLL of −27.82 dB by only optimizing the ring radius and strictly constraining the element number on the corresponding ring. HA [19] obtained the best PSLL of −27.92 dB by both optimizing the ring radius and the element number on the ring. The best PSLL obtained by the CSSA is −29.16 dB when the number of rings $N_r = 7$ and the total amount of elements $N_t = 161$, which is 1.34 dB lower than when using GA and 1.24 dB lower than when using HA. Figure 4(a) shows the best element distribution of an acquired array. The radius of each ring is 0.59λ, 1.13λ, 1.66λ, 2.26λ, 3.01λ, 3.80λ, and 4.70λ. The corresponding number of elements is 7, 13, 19, 25, 32, 29, and 35. Figure 4(b) depicts the radiation pattern in the $\varphi = 0$ plane, while Figure 4(c) depicts the radiation pattern in three dimensions. Finally, the total computation time for this example to complete a single trial is approximately 381 s.

4.3. Example C: $R = 4.3\lambda$. In the third example, the proposed CSSA method has been used to carry out a synthesis experiment with an array radius of 4.3λ. The best array is built with 147 elements distributed in 7 rings, and the best element distribution of the obtained array is shown in Figure 5(a). Figure 5(b) shows the comparison of array radiation patterns between HA and CSSA in the $\varphi = 0$ plane. It can be concluded that the CSSA has obtained a 1.13 dB lower PSLL than HA and that the 3 dB main beamwidth obtained by the CSSA is slightly higher than that obtained by

Table 1: Performance comparison between the proposed CSSA and some state-of-the-art algorithms.

Aperture (λ)	Method	N_r	N_t	PSLL (dB)	Directivity coefficient (dB)	3 dB beamwidth
$R = 4.98$	GA [13]	6	201	−22.94	27.38	0.1012
	MGA [14]	10	201	−23.74	—	—
	HA [19]	8	201	−29.03	29.18	0.1126
	CSSA	8	192	−30.08	29.09	0.1129
$R = 4.7$	GA [13]	6	142	−27.82	28.89	0.1118
	HA [19]	7	142	−27.92	28.51	0.1126
	CSSA	7	161	−29.16	29.60	0.1137
$R = 4.3$	HA [19]	7	134	−29.07	28.18	0.1224
	CSSA	7	147	−30.20	28.81	0.1256

Table 2: Ring radius and the number of elements in the ring achieved by CSSA.

Aperture (λ)		$r_n(\lambda)$ and N_n							
		1	2	3	4	5	6	7	8
$R = 4.98$	r_n	0.50	1.00	1.50	2.00	2.61	3.34	4.17	4.98
	N_n	6	12	18	21	31	37	31	35
$R = 4.7$	r_n	0.59	1.13	1.66	2.26	3.01	3.80	4.70	—
	N_n	7	13	19	25	32	29	35	—
$R = 4.3$	r_n	0.50	1.00	1.50	2.00	2.66	3.45	4.30	—
	N_n	6	12	16	22	31	28	31	—

HA. Figure 5(c) depicts the corresponding 3-D view of the radiation pattern. Finally, the total computation time for this example to complete a single trial is approximately 377 s.

Finally, Table 1 presents the performance comparison results between the proposed CSSA and some state-of-the-art algorithms when $R = 4.98\lambda$, 4.7λ, and 4.3λ, which include the number of rings N_r, the total number of elements N_t, the best PSLL, the direction coefficient, and the 3 dB beamwidth. Table 2 illustrates the radius r_n and the number of elements N_n on the corresponding ring acquired by the CSSA. Numerical examples show that the CSSA is able to obtain lower PSLL values under the same fitness conditions.

Based on the above analysis results, it can be concluded that optimizing the array element positions by the CSSA can obtain a better PSLL suppression effect while maintaining a higher directivity coefficient and a narrower 3 dB beamwidth. In the three simulation examples, the proposed method has preferable efficiency and good convergence. In addition, the comparison of the proposed method with state-of-the-art algorithms demonstrates its superiority in array sparse optimization.

5. Conclusion

We proposed an effective method for the synthesis of sparse CRA with multiple constraints, which effectively achieved SLL suppression of equally uniformly excited CRA. The numerical results demonstrate that the proposed CSSA method achieved a better SLL suppression effect than other methods when the apertures were fixed. Moreover, the proposed method has the potential to solve other array models with multiple constraints, such as rectangular planar arrays and conformal unequally spaced arrays, which have a certain reference value for the optimal design and engineering applications of array antennas in the future.

Data Availability

The data used to support the findings of this study are available from the corresponding author upon request.

Conflicts of Interest

The authors declare that they have no conflicts of interest.

Acknowledgments

This work was supported in part by the National Natural Science Foundation of China under Grant no. 62271011 and the Chongqing Postgraduate Research and Innovation Project under Grant no. CYS21321.

References

[1] O. M. Bucci, S. Perna, and D. Pinchera, "Interleaved isophoric sparse arrays for the radiation of steerable and switchable beams in satellite communications," *IEEE Transactions on Antennas and Propagation*, vol. 65, no. 3, pp. 1163–1173, 2017.

[2] Y. Aslan, A. Roederer, and A. Yarovoy, "Synthesis of optimal 5G array layouts with wide-angle scanning and zooming ability for efficient link setup and high-QoS communication," *IEEE Antennas and Wireless Propagation Letters*, vol. 19, no. 9, pp. 1481–1485, 2020.

[3] U. Singh and T. S. Kamal, "Synthesis of thinned planar concentric circular antenna arrays using biogeography-based optimisation," *IET Microwaves, Antennas & Propagation*, vol. 6, no. 7, pp. 822–829, 2012.

[4] A. Kedar, "Deterministic synthesis of wide scanning sparse concentric ring antenna arrays," *IEEE Transactions on Antennas and Propagation*, vol. 67, no. 12, pp. 7387–7395, 2019.
[5] Z. Shi and Z. Feng, "A new array pattern synthesis algorithm using the two-step least-squares method," *IEEE Signal Processing Letters*, vol. 12, no. 3, pp. 250–253, 2005.
[6] X. Tian, H. Chen, M. He, and W. Wang, "Fast beampattern synthesis algorithm for flexible conformal array," *IEEE Signal Processing Letters*, vol. 29, pp. 2417–2421, 2022.
[7] R. Rajamäki and V. Koivunen, "Sparse active rectangular array with few closely spaced elements," *IEEE Signal Processing Letters*, vol. 25, no. 12, pp. 1820–1824, 2018.
[8] N. Jin and Y. Rahmat-Samii, "Advances in particle swarm optimization for antenna designs: real-number, binary, single-objective and multiobjective implementations," *IEEE Transactions on Antennas and Propagation*, vol. 55, no. 3, pp. 556–567, 2007.
[9] W. P. M. N. Keizer, "Synthesis of thinned planar circular and square arrays using density tapering," *IEEE Transactions on Antennas and Propagation*, vol. 62, no. 4, pp. 1555–1563, 2014.
[10] R. Willey, "Space tapaering of linear and planar arrays," *IRE Transactions on Antennas and Propagation*, vol. 10, no. 4, pp. 369–377, 1962.
[11] T. M. Milligan, "Space-tapered circular (ring) array," *IEEE Antennas and Propagation Magazine*, vol. 46, no. 3, pp. 70–73, 2004.
[12] Y. Jiang and S. Zhang, "An innovative strategy for synthesis of uniformly weighted circular aperture antenna array based on the weighting density method," *IEEE Antennas and Wireless Propagation Letters*, vol. 12, pp. 725–728, 2013.
[13] R. L. Haupt, "Optimized element spacing for low sidelobe concentric ring arrays," *IEEE Transactions on Antennas and Propagation*, vol. 56, no. 1, pp. 266–268, 2008.
[14] K. Chen, H. Chen, L. Wang, and H. Wu, "Modified real GA for the synthesis of sparse planar circular arrays," *IEEE Antennas and Wireless Propagation Letters*, vol. 15, pp. 274–277, 2016.
[15] B. V. Ha, M. Mussetta, P. Pirinoli, and R. E. Zich, "Modified compact genetic algorithm for thinned array synthesis," *IEEE Antennas and Wireless Propagation Letters*, vol. 15, pp. 1105–1108, 2016.
[16] Q. Guo, Y. Wang, D. Yuan, J. Li, and T. Yu, "Optimization of sparse concentric ring arrays based on multiple constraints," *IEEE Antennas and Wireless Propagation Letters*, vol. 19, no. 5, pp. 781–785, 2020.
[17] Y. Li, F. Yang, J. Ouyang, Z. Nie, and H. Zhou, "Synthesis of nonuniform array antennas using particle swarm optimization," *Electromagnetics*, vol. 30, no. 3, pp. 237–245, 2010.
[18] A. Chatterjee, G. K. Mahanti, and P. R. S. Mahapatra, *Optimum Ring Spacing and Interelement Distance for Sidelobe Reduction of a Uniform Concentric Ring Array Antenna Using Differential Evolution Algorithm*, IEEE International Conference on Communication Systems, Singapore, 2010.
[19] Q. Guo, C. Chen, and Y. Jiang, "An effective approach for the synthesis of uniform amplitude concentric ring arrays," *IEEE Antennas and Wireless Propagation Letters*, vol. 16, pp. 2558–2561, 2017.
[20] J. Xue and B. Shen, "A novel swarm intelligence optimization approach: sparrow search algorithm," *Systems Science & Control Engineering*, vol. 8, no. 1, pp. 22–34, Jan.2020.
[21] Q. Liu, Y. Zhang, M. Li, Z. Zhang, N. Cao, and J. Shang, "Multi-UAV path planning based on fusion of sparrow search algorithm and improved bioinspired neural network," *IEEE Access*, vol. 9, pp. 124670–124681, 2021.
[22] J. Yuan, Z. Zhao, Y. Liu et al., "DMPPT control of photovoltaic microgrid based on improved sparrow search algorithm," *IEEE Access*, vol. 9, pp. 16623–16629, 2021.